Reaction $e + p \rightarrow e + p + \omega$

J. T. Linnemann,[a] L. A. Ahrens,[b] K. Berkelman, D. G. Cassel, C. T. Day,[c] B. G. Gibbard,[b] D. J. Harding,[d] D. L. Hartill, J. W. Humphrey,[b] T. J. Killian,[e] J. S. Klinger,[d] E. A. Treadwell,[d] and D. H. White[b]

Laboratory of Nuclear Studies, Cornell University, Ithaca, New York 14853

(Received 14 April 1978)

The production of the ω meson by virtual photons has been measured as a function of Q^2 and W. The ratio of ω production to ρ^0 production is independent of Q^2 in contrast to indications at lower values of W.

In this paper we present results on the production of the ω by virtual photons on protons. The production cross sections for vector mesons are known to decrease with Q^2 from their photoproduction values. In this experiment we have extended the range of Q^2 and W over which this variation has been measured for the ω.[1] The production of the ω by virtual photons at energies well above threshold has been understood in terms of a model including s-channel effects, one-pion exchange, and diffraction.[2] The larger kinematic range available in this experiment provides a more stringent test of these ideas.

A schematic diagram of the apparatus in which these measurements were made is shown in Fig. 1. We expect to describe this apparatus in detail in a later publication. An electron beam of energy 11.5 GeV was extracted from the Cornell Electron Synchrotron and focused on a 7.5-cm-long liquid-hydrogen target placed inside the gap of the magnet with an 0.8-T field. Scattered electrons were identified in the lead-scintillator-sandwich shower counter by matching the amplitude of the signal with the reconstructed momentum. In the event sample described here, all the charged particles were detected and their momenta reconstructed using the 22 000-wire multiwire proportional chambers shown in the diagram. The position resolution achieved is consistent with the 1.5-mm wire spacing. On each side of the center line, seven planes measured horizontal coordinates (bend direction), six measured vertical coordinates, and four measured coordinates at 30° to the vertical to resolve ambiguities. In addition, hadron tracks reconstructed in the chambers had a geometric probability of 0.6 of being detected in the scintillation and water Čerenkov counters. The time of flight from the target and the pulse height in the Čerenkov counters were used to aid in the identification of the particles.

The events were derived from a sample of about 5×10^6 particles which triggered the electron counter and for which a corresponding negative track was reconstructed. For these electrons, the square of the four-momentum transfer, Q^2, was between 0.5 GeV^2 and 4.0 GeV^2. The center-of-mass energy of the virtual-photon–proton system, W, varied between 1.4 and 4.0 GeV. Events of appropriate topology were then subjected to kinematic fits and those events selected for which there was a good fit to the one constraint hypothe-

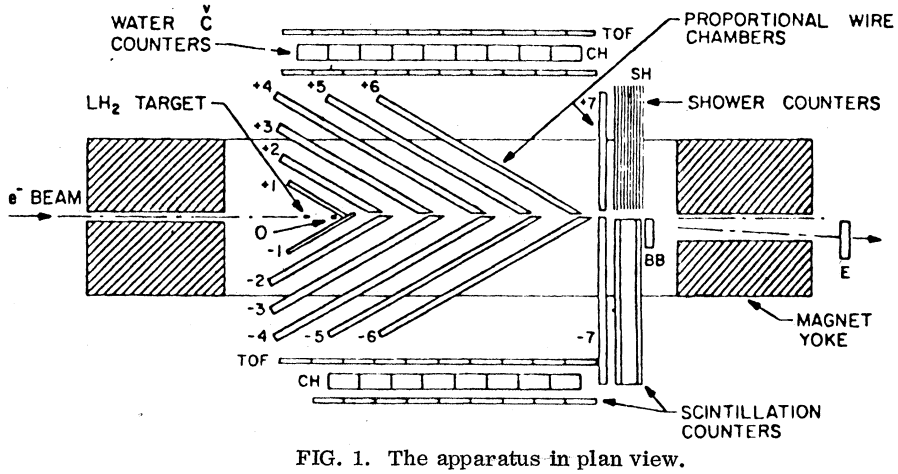

FIG. 1. The apparatus in plan view.

sis,

$$e+p \rightarrow e+p+\pi^+ +\pi^- +\pi^0 . \quad (1)$$

The particles that were detected in the time-of-flight counters and the water Čerenkov counters were checked for consistency between the prediction of the kinematic fit and the identifications inferred from the counters.[3] Events which satisfied the four-constraint hypothesis,

$$e+p \rightarrow e+p+\pi^+ +\pi^- , \quad (2)$$

were removed from the sample. All hypotheses with kaons in the final states were ignored, since these events do not simulate an ω and only contribute to the background. They are not expected to be a major source of background.[4,5] After these cuts, the combination that had the smallest value for the sum of the kinematic χ^2 and the counter χ^2 was selected.

The $\pi^+\pi^-\pi^0$ invariant-mass distribution is shown in Fig. 2 with the ω signal clearly visible. The distribution has been fitted with a smoothly varying background and a Gaussian peak at 785 ± 5 MeV/c^2. This value is consistent with the accepted mass of the ω, and we have fixed this mass at 783 MeV/c^2 in further analysis. The ω cross sections were extracted by fitting with a Gaussian with a smooth background in the mass range 723–843 MeV/c^2. The total number of incident electrons was measured with a secondary-emission quantameter. The detection efficiency for ω mesons was estimated by the following method. The efficiency of the individual proportional chambers was estimated from the strike distributions of the detected tracks. Data were taken with the enabling trigger at random times in ths spill so that the distribution of "background strikes" was established. A sample of ω-meson events was created assuming a production cross section that was approximately consistent with the final results reported here. These events were used to produce a strike distribution in the chambers through algorithms that reporduced the data of typical tracks including the measured efficiency. The "background strikes" were added and this composite data subjected to the normal analysis stream, with all the cuts that were used on the main data sample. The ratio of ω events that remained, to those created originally, gave a detection efficiency. This detection efficiency does not vary noticeably in the Q^2 and W ranges in which sensible ω data exist in this experiment. In addition, two-prong events were subjected to the same analysis and the elastic-scattering cross section was determined. The cross section agreed within errors with the accepted value. The ρ^0 quasielastic cross section was similarly determined from the four-prong sample. The cross section agreed with that reported by Joos *et al.*[6] in the regions of W and Q^2 that were common to both experiments.

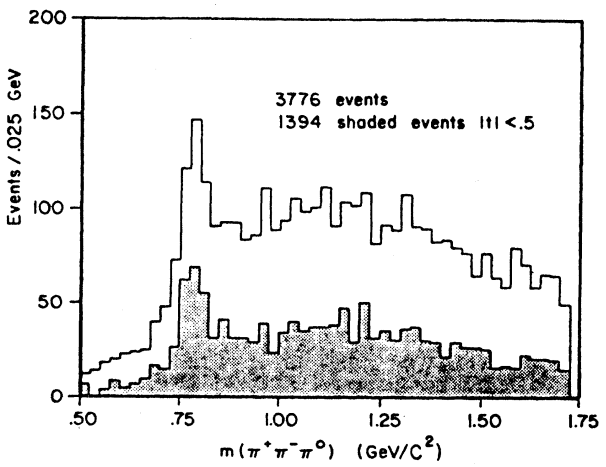

FIG. 2. The $\pi^+\pi^-\pi^0$ invariant-mass distribution for $e+p \rightarrow e+p+\pi^+ +\pi^- +\pi^0$ events.

In Fig. 3 we show the variation of the total ω virtual-photon–proton production cross section. A rapid variation with Q^2 is seen in contrast with the data of Joos *et al.*[1] We have also plotted the photoproduction cross section for this range of W,[7] and, to guide the eye, we have drawn a curve of the function

$$\sigma_\omega(Q^2) = \sigma_\omega(0) m_\omega^4/(Q^2+m_\omega^2)^2 . \quad (3)$$

In Fig. 3 we have also plotted the function

$$\sigma(Q^2) = \sigma(0)\exp B[t_{\min}(Q^2) - t_{\min}(0)].$$

It is clear that the effect of $t_{\min}$ in this range of W and Q^2 is large; following convention we have chosen not to correct these data for this effect.

In this region of Q^2 and W the production of the ω and ρ^0 are thought to be closely related. In Fig. 4 we show the ratio of these cross sections, calculated from the ρ^0 production values measured in this experiment.[8] At the intermediate value of W, our data agree with earlier data for the production of ω in μp interactions.[9] From our data, we conclude that there is no substantial variation of the ratio $\sigma_\omega/\sigma_\rho$ with Q^2. We have examined the differential cross section for ω production as a function of $t-t_{\min}$; we see exponential behavior with an average slope $B = 6.1 \pm 0.8$ GeV^{-2}, compared to the photoproduction

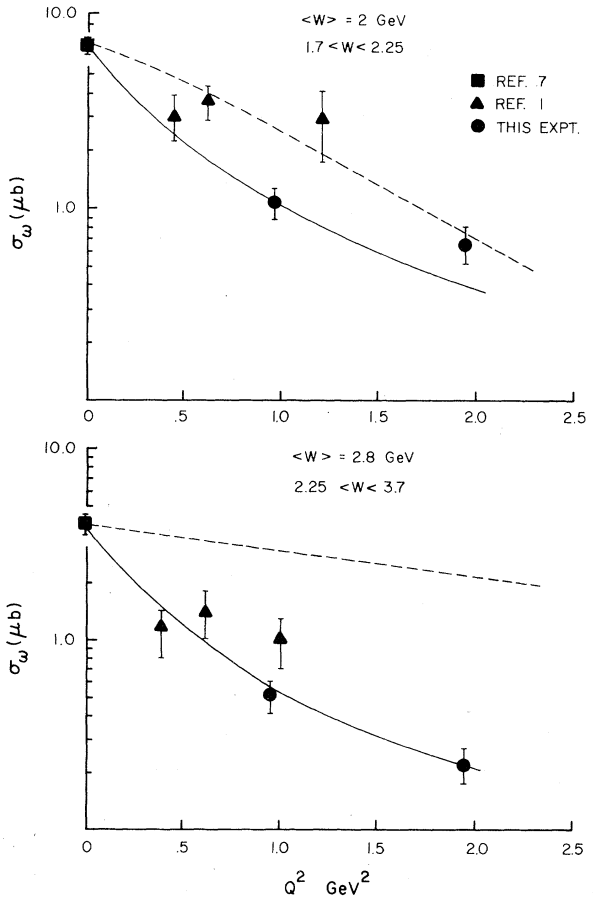

FIG. 3. The virtual-photon–proton cross section for ω production as a function of Q^2 for two ranges of W. We have also plotted the function (solid curve) $\sigma(Q^2) = \sigma(0) m_\omega^4/(Q^2+m_\omega^2)^2$ and (dashed curve) $\sigma(Q^2) - \sigma(0) \times \exp B[t_{\min}(Q^2) - t_{\min}(0)]$.

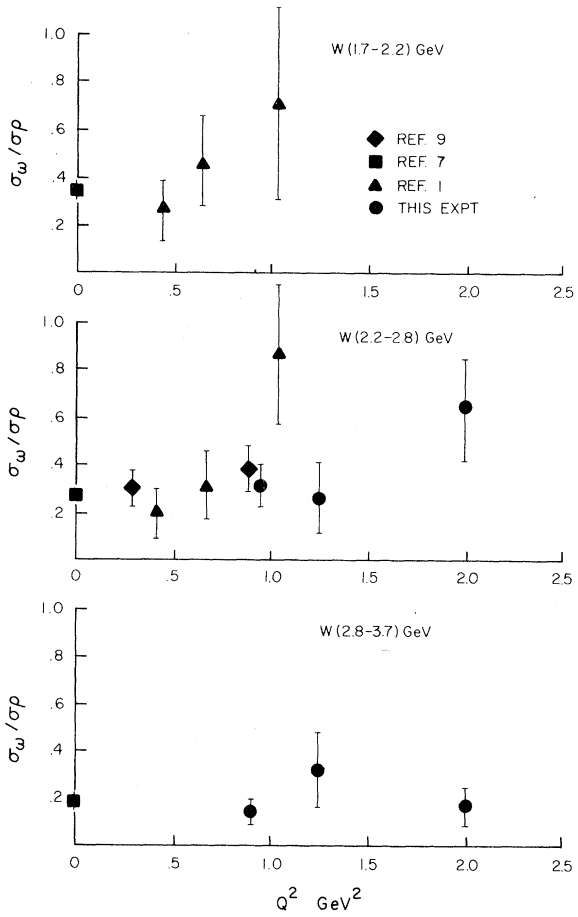

FIG. 4. The ratio of the ω production for three ranges of W.

value of 8.4 ± 1.2 GeV^{-2} in this range of W.[7]

The model described by Joos *et al.*[1] included s-channel effects and a contribution due to one-pion exchange. In the higher-energy range of this experiment ω production is entirely peripheral. The photoproduction data of Ballam *et al.*[7] shows a pion-exchange contribution that is 0.55 of the total in the range $2.2 < W < 2.8$ GeV and 0.40 in the range $2.8 < W < 3.7$ GeV. Since the ratio of $\sigma_\omega/\sigma_\rho$ remains independent of Q^2 in both these ranges of W, we deduce that the Q^2 variation of the one-pion-exchange (OPE) contribution and that from diffraction effects must be similar. For example, if the OPE contribution were to vary as $\sigma_{\mathrm{OPE}}(Q^2) = \sigma_{\mathrm{OPE}(0)} m_\omega^2/(Q^2 - m_\omega^2)$ then the ratio $\sigma_\omega/\sigma_\rho$ would change by a factor of 4 between $Q^2 = 0$ and $Q^2 = 1$ GeV^2. We conclude then that when the energy is high enough that s-channel effects are unimportant, the two processes identified in ω production and also the single process in the production of the ρ^0 have the same variation with Q^2.

This work was supported in part by the National Science Foundation.

---

[a]Present address: Rockefeller University Group, CERN, 1211 Geneva 23, Switzerland.
[b]Present address: Brookhaven National Laboratory, Upton, N. Y. 11973.
[c]Present address: Lawrence Berkeley Laboratory, Berkeley, California 94702.
[d]Present address: Fermilab, P. O. Box 500, Batavia, Illinois 60510.
[e]Present address: NP Division, CERN, 1211 Geneva 23, Switzerland.

[1]P. Joos *et al.*, Nucl. Phys. B122, 365 (1977), B113, 53 (1976).
[2]H. Fraas, Nucl. Phys. B36, 191 (1972).
[3]D. J. Harding, Ph.D. thesis, Cornell University,

1978 (unpublished); E. A. Treadwell, Ph.D. thesis, Cornell University, 1978 (unpublished).
[4]J. F. Martin *et al.*, Phys. Rev. Lett. 40, 283 (1978).
[5]C. T. Day, Ph.D. thesis, Cornell University, 1978 (unpublished).
[6]P. Joos *et al.*, Nucl. Phys. B113, 53 (1976).
[7]J. Ballam *et al.*, Phys. Rev. D 5, 545 (1972).
[8]L. A. Ahrens, Ph.D. thesis, Cornell University, 1978 (unpublished).
[9]J. Ballam *et al.*, Phys. Rev. D 10, 765 (1974).

Violations of SU(6) Selection Rules from Quark Hyperfine Interactions

Nathan Isgur
Department of Physics, University of Toronto, Toronto M5S 1A7, Canada

and

Gabriel Karl
Department of Physics, University of Guelph, Guelph N1G 2W1, Canada

and

Roman Koniuk
Department of Physics, University of Toronto, Toronto M5S 1A7, Canada
(Received 18 September 1978)

The decay amplitudes for $D_{15}\to p\gamma$, the amplitude for $D_{05}\to \bar{K}N$, and the charge radius of the neutron are zero in the SU(6) limit, but are observed to be nonzero. We show that all of these SU(6)-violating effects can be understood quantitatively in terms of the admixtures of excited-state configurations in the nucleon expected on the basis of color hyperfine interactions. In particular, the admixture of ^2S_M (i.e., $[\underline{70},0^+]$) with an amplitude of about $-\frac{1}{4}$ is central to understanding all three effects.

In the consideration of baryon decays[1] within the framework of the SU(6) quark model or $SU(6)_W$, two simple selection rules relevant to the negative-parity P-wave baryons emerge: Decays of the types

$$N\,{}^4P_M\to p\gamma \tag{1}$$

and

$$\Lambda\,{}^4P_M\to \bar{K}N \tag{2}$$

are forbidden[2] (our notation is $X^{2S+1}L_\sigma$, where $\sigma=S, M, A$ is the symmetry of the spatial wave function). These selection rules are most clearly tested in the specific decays $D_{15}(1670)\to p\gamma$ and $D_{05}(1830)\to \bar{K}N$ since in these cases mixing with other members of the $[\underline{70},1^-]$ multiplet is impossible. In both cases the selection rule is found to be approximately satisfied; for example, the branching ratio for $\Lambda(\frac{5}{2}^-;1830)\to\bar{K}N$ is less than 10%. Nevertheless, in both cases violations of the selection rule are clear and well established. Columns 1 and 3 of Table I summarize the situation.

Recent work on quark models[8,9] has provided a considerable body of evidence in favor of the idea that violations of SU(6) symmetry of another kind —those responsible for the mass splittings and mixings of the SU(6) multiplets—can be explained in terms of color hyperfine interactions between quarks. These are interactions which can arise from one-gluon exchange which are analogous to

TABLE I. Violations of some SU(6) rules.

Quantity	SU(6) (Relative values)	This calculation (Relative values)	Experiment (Various units)
$A_{3/2}^n(D_{15}\to n\gamma)$	$-\alpha$	$-\alpha$	-60 ± 33 [a]
$A_{1/2}^n(D_{15}\to n\gamma)$	-0.71α	-0.71α	-33 ± 25 [a]
$A_{3/2}^p(D_{15}\to p\gamma)$	0	$+0.31\alpha$	$+20\pm13$ [a]
$A_{1/2}^p(D_{15}\to p\gamma)$	0	$+0.22\alpha$	$+19\pm14$ [a]
$A(D_{15}\to \bar{K}N)$	β	β	$+0.41\pm0.03$ [b]
$A(D_{05}\to \bar{K}N)$	0	-0.28β	-0.09 ± 0.04 [c]
$\langle\sum e_i r_i^2\rangle_p$	γ	γ	$+0.82\pm0.02$ [d]
$\langle\sum e_i r_i^2\rangle_n$	0	-0.16γ	-0.12 ± 0.01 [e]

[a]Ref. 3.
[b]Refs. 3 and 4.
[c]Refs. 4 and 5.
[d]Ref. 6.
[e]Ref. 7.